

Article ID: 1006-8775(2010) 03-0231-07

AN EMPIRICAL ORTHOGONAL FUNCTION ANALYSIS FOR THE WAVE TRAINS IN EAST ASIAN SUMMER

WANG Ya-fei (王亚非)¹, HE Jin-hai (何金海)², LI Yan (李 琰)¹, ZHU Li-juan (祝丽娟)¹

(1. State Key Laboratory of Severe Weather Chinese Academy of Meteorological Sciences, Beijing 100081 China; 2. Nanjing University of Information Science & Technology, Nanjing 210044 China)

Abstract: This study examines the wave trains at 500 hPa occurring in East Asian summer by using the Empirical Orthogonal Function (EOF) analysis as a diagnostic tool. The results are summarized as follows: (1) A wave train pattern (OKJ pattern) originating from the upstream areas of the Sea of Okhotsk to the subtropical regions could display its strong signal in early and middle summer. The OKJ pattern is clearly recognized in the first EOF component in Eurasia. (2) The other wave train pattern originating from the Philippines via Japan to North America (the P-J pattern) shows quite strong signals in the whole summer. Although the P-J pattern is described as the second EOF component around the area from East Asia to Northeast Pacific Ocean, the variance contribution is the same as that of OKJ pattern in the first EOF component. (3) The composite analyses indicate that the OKJ and P-J wave trains could coexist to some extents.

Key words: wave trains; East Asian summer; EOF analysis; teleconnection; 500 hPa

CLC number: P424

Document code: A

doi: 10.3969/j.issn.1006-8775.2010.03.004

1 INTRODUCTION

The concept of teleconnection was firstly proposed by Walker^[1] who used it to explain the southern oscillation. And then, Wallace and Gutzler^[2] obtained five well-known teleconnection patterns by calculating one-point correlation maps for the Northern Hemisphere in winter. Hoskins and Karoly^[3] linked the teleconnection with the Rossby wave propagation and pointed out that the five teleconnection patterns might be associated with the stationary Rossby wave propagation. The Rossby wave generally propagates mainly along a route linking individual correlation centers in the one-point correlation map (the great circle path). The weather in the related regions can be greatly influenced by the energy dispersion. For example, large variations in weather that could be related to the Rossby wave propagation were observed in the hot or cold summer in Japan (Nitta^[8]; Wang^[4]). There are generally two kinds of wave trains that could induce large weather variations in East Asian summer. One is the propagation of the stationary wave from higher latitudes to lower latitudes (hereafter referred to as the "OKJ wave", shown in Fig. 9 of Wang^[4]), which

was first proposed by Wang and was later verified and studied further by Kato, Nakamura and Ogi^[4-7]. The wave route is generated from one point correlation between outgoing long wave radiation (OLR) at 30°N, 150°E and the geopotential height at 500 hPa (Z500) in June. The connecting line of the correlation centers can be approximately recognized as the great circle path. The successive correlation centers are located at the Sea of Okhotsk, off the east coast of Japan and the subtropical region in Southeast Japan. Wang^[4] pointed out that the stimulation of this stationary Rossby wave propagation is usually accompanied with the development of a blocking high in the Sea of Okhotsk, and a southward shift of Meiyu front by deepening the cyclonic systems in the south of Japan. This finding exemplifies how the impact of the Rossby wave propagation from higher latitudes exerted on the weather around lower latitudes. The other Rossby wave train (hereafter referred to as the "P-J wave") has been studied further. Correlation maps are made between OLR at 15°N, 140°E and Z500 in August, with the correlation centers originating from the Philippin Sea across the Pacific to form a great circle path (figure not shown). Nitta^[8] pointed out that the convective activity

Received date: 2009-10-15; **revised date:** 2010-04-28

Foundation item: China-Japan intergovernmental cooperation program of the JICA (2009LASWZF04), Program of Ministry of Science and Technology of China (2009DFB20540)

Biography: WANG Ya-fei, Ph.D., mainly studying the mechanisms of variation of atmospheric circulation. E-mail for corresponding author: yfwang@cams.cma.gov.cn

around the Philippines in midsummer plays a role in generating the northeastward P-J wave propagation, which could probably result in the hot weather in Japan. Huang^[9] suggested that persistent P-J wave propagation can bring drought to eastern China. Although the one-point correlation map shows that the OKJ wave mainly appears in early summer and the P-J wave in midsummer, cases of emergence of OKJ waves in midsummer and the P-J wave in early summer cannot be excluded (e.g. in 1998). Because of the strong impact of the two wave trains on the synoptic atmospheric circulation in East Asia, it is of great importance to investigate the occurrence frequency of the wave trains essential to the prediction of the summer climate in East Asia. Thus, our study is aimed at evaluating the respective proportion of the occurrence of two wave trains in the whole summer by using the Empirical Orthogonal Function (EOF) analysis as a diagnostic tool.

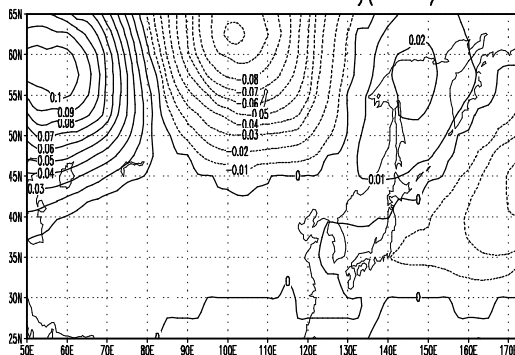
2 DATA

The U.S. NCEP/NCAR (National Centers for Environmental Prediction/National Center for Atmospheric Research) global atmospheric reanalysis dataset is the primary dataset. We used pentad (June–August 1979–1998) 500-hPa geopotential height and pentad (August 1979–1998) OLR set onto a 2.5° latitude/longitude grid.

3 OKJ PATTERN IN SUMMER

To examine whether the occurrence of the OKJ pattern is normal in summer, we applied the EOF analysis to the pentad geopotential height at 500 hPa in summer from 1979 to 1998. The data used for EOF analysis are the anomalies from the zonal mean that follow the wave flux theory proposed by Plumb^[10]. Special attention was paid to the large area of East Asia and extensions to the upstream area, because the Rossby wave usually propagates from farther upstream regions. Two overlapping periods are chosen to represent the prophase and anaphase of summer, i.e.

EOF I distribution June to July(79–98)



June to July (Pentads 31–42) and July to August (Pentads 37–48). A correlation matrix was used to calculate a set of the eigenvectors, eigenvalues and time coefficients of each mode.

Figures 1 and 2 show the spatial patterns of the first two components for June to July and July to August, respectively. The pentad cumulative contributions (%) of the first three eigenvectors in Pentads 31–42 and Pentads 37–48 provide 44.8% and 44.7% of the total variance, respectively (Table 1). The statistical significance of the variance associated with each EOF is verified using the selection rules of the Monte Carlo technique (Overland and Preisendorfer^[11]). We calculated 100 sets of eigenvalues for 100 fields of uncorrelated random numbers, giving a 95% confidence level for each order of eigenvalue. To be significant, the current variances must be significantly greater than those in the uncorrelated field. The variances of the first three eigenvalues exceed the confidence level by large margin. As shown in Fig. 1a, the first pattern of the Pentads 31–42, which accounts for 17.7% of the total variance, displays a wave train-like pattern at higher latitudes. The negative centers are located at the point (62.5°N, 100°E, around Tula in Russia) and the area off the east coast of Japan (42.5°N, 170°E). The positive ones are located around the Sea of Okhotsk (57.5°N, 147.5°E) and at the point (57.5°N, 55°E, to the west of the Ural Mountains). This distribution is closely related to the OKJ pattern, which is shown in Fig. 9 of Wang^[4]. Several degrees of phase drift in longitude are found between this figure and Fig. 1a. However, the former seems to reflect the activity of somewhat smaller-scale systems. The pattern of the second component, accounting for 15.2% of the total, shows a north-south oscillation mainly occurring west of 110°E, as shown in Fig. 3b. In contrast, a large negative center is located at (50°N, 90°E) and a large positive one at (55°N, 165°E), which indicates an east-west seesaw during the period (not shown).

EOF II distribution June to July(79–98)

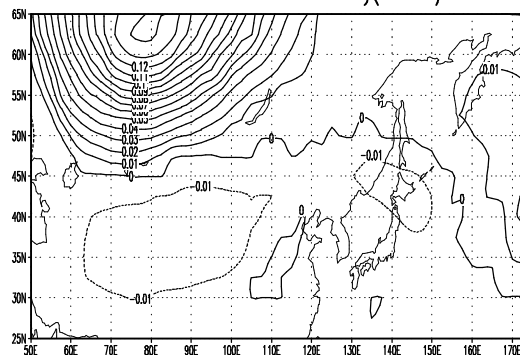


Fig. 1. Distribution of the previous two EOF eigenvectors during June–July (Pentads 31–42) of Z500

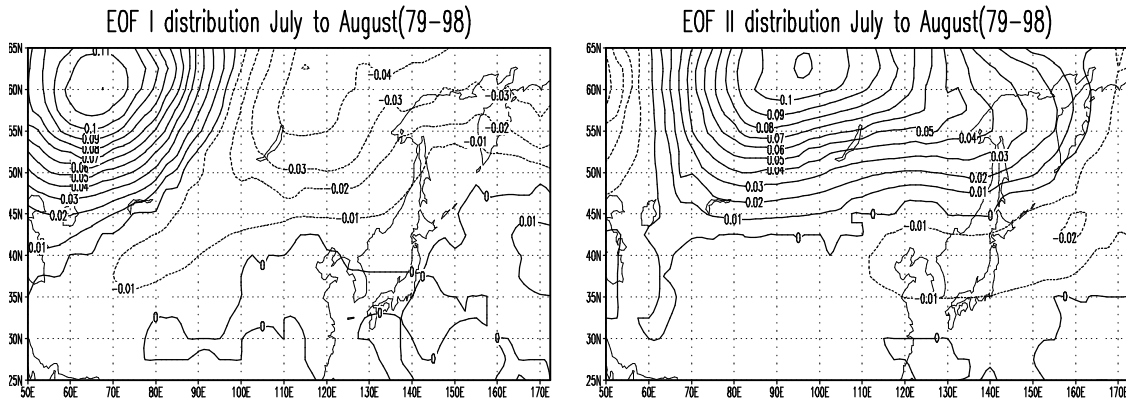


Fig. 2. Same as Fig. 1 except for the distribution during July–August (Pentads 37–48)

Table 1. Variance contribution of the previous three eigenvectors in Eurasia

Eigenvector	EOF I	EOF II	EOF III
June–July	0.1774	0.1525	0.1186
July–August	0.1899	0.1503	0.1075

On the other hand, the EOF analysis for the July to August period shows a similar but nevertheless different pattern to that in June to July. A wave train-like pattern in Fig. 2a (c: 19.0%) dominates at higher latitudes. The route linking with each correlation center in Fig. 2a almost coincides with that in Fig. 1a, but the correlation centers shift eastward about 10-20 degrees in longitude and the wave length is much larger compared with that in Fig. 1a. The second component, accounting for 15.0% of the total, shows a large positive value at (62.5°N, 97.5°E) and a weak negative center at (42.5°N, 160°E) (Fig. 2b), which basically represents a southeast-northwest seesaw somewhat similar to that in Fig. 1b. The third component (c: 10.75%) also shows a wave train pattern and this pattern seems to be the OKJ pattern, although this wave train occurs at higher latitudes than the OKJ pattern in early summer (not shown).

As shown above, the OKJ-like wave train pattern dominates in the first EOF component from June to July and it is the third component from July to August. In order to investigate this pattern, we will concentrate on the first component of the analysis in Pentads 31-42 (June to July) in this section. Fig. 3 shows the normalized time series of score of the first EOF component in Pentads 31–42, which fluctuated mainly from +2 to –2. The composites are made according to the extent to which the value of the coefficient is over 1.0 or below –1.0.

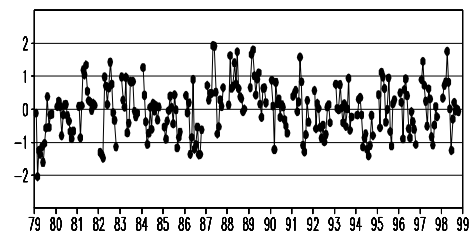


Fig. 3. Evolution of the coefficient of the EOF I during Pentads 31–42 (June to July) of Z500 in 1979–1998

Figures 4a & 4b show the composites of the horizontal wave activity flux and geopotential height at 500 hPa during the pentads when the score is over 1.0 (Fig. 4a) and below –1.0 (Fig. 4b), respectively. The wave activity flux is calculated according to Plumb^[10], using a method that indicates the magnitude and direction of the stationary wave propagation. The formula of the horizontal wave flux is as follows:

$$F = \begin{pmatrix} F_\lambda \\ F_\phi \end{pmatrix} = \frac{p}{p_s} \cos\phi \times \begin{pmatrix} v'^2 - \frac{1}{2\Omega a \sin 2\phi} \frac{\partial(v'\Phi')}{\partial\lambda} \\ -u'v' + \frac{1}{2\Omega a \sin 2\phi} \frac{\partial(u'\Phi')}{\partial\lambda} \end{pmatrix} \quad (1)$$

where the u' and v' of wind are zonal anomalies after the application of geostrophic approximation, ϕ' is the zonal anomaly of geopotential height, Ω and a are the angular velocity of rotation and radius of the earth, respectively (refer to Wang and Yasunari^[12] for detail). In a positive phase of EOF1, a blocking-like high is established around the Sea of Okhotsk and two troughs are found on its eastern and western sides (Fig. 4a). The eastward wave activity flux dominates at high latitudes from Europe to East Asia, but turns southeastward around the Sea of Okhotsk. The strong flux (maximum: about 65 m² s⁻²) progresses southeastward to 30°N around Japan and the sea area to its east. This phenomenon is the same as that discussed by Wang and Yasunari^[12] although the data they used were limited to June only. Therefore, the occurrence of Rossby wave propagation from higher latitudes to lower latitudes in the mid-summer is not

rare. Note that the western edge of the ridge line of the subtropical high (5880 contour line) is located around 20°N. This indicates that the western edge of the subtropical high is located in a further southward area

than normal, whose situation is similar to the summers of decaying El Niño shown by Wang et al.^[13] They pointed out that this circulation pattern is associated with a strong East Asian summer monsoon.

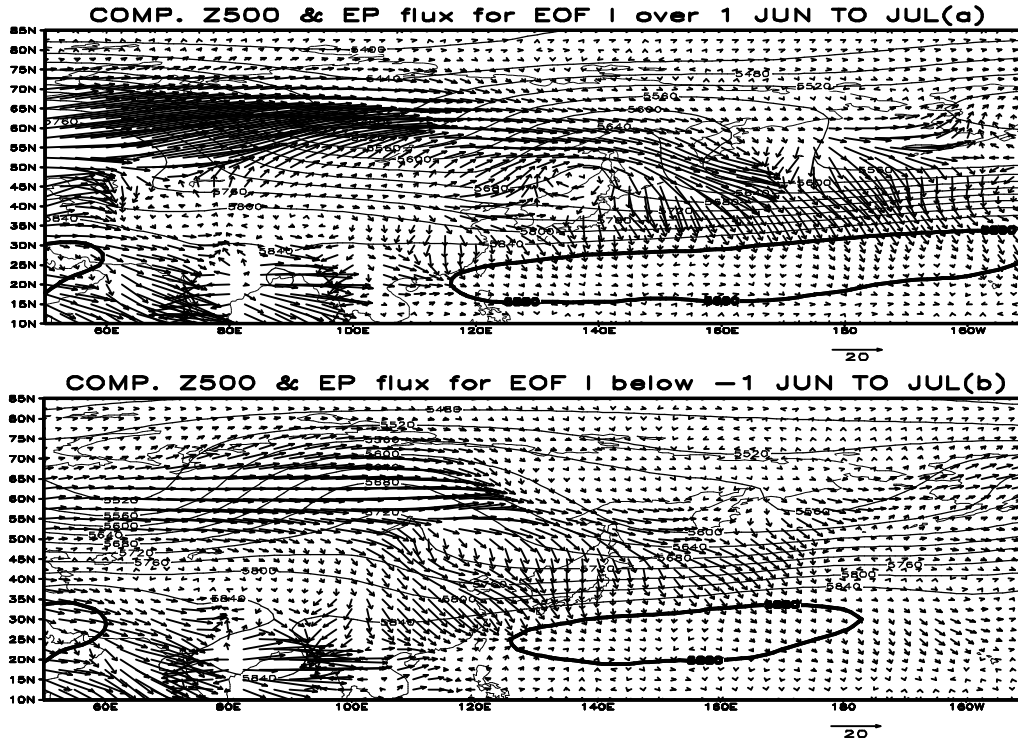


Fig. 4. Horizontal wave activity flux and Z500 for the pentads over 1.0 (a) and below -1.0 (b) of the time coefficient of the first component. The line at 5800 gpm is in bold.

On the other hand, the circulation pattern in a negative phase of EOF1 (Fig. 4b) is almost the opposite of that in a positive phase. A strong ridge is located over the Lake of Baikal and the two troughs are on its western and eastern sides (of the Sea of Okhotsk). The eastward wave flux still dominates in higher latitudes while the southeastward one extends from the Lake Baikal to an extensive area that covers China, Korea, and Japan. Although the sign of the anomalies is reversed to the positive phase of EOF1, the direction of the wave activity flux for both phases changes little. The western edge of the subtropical high (5880 contour line) moves northward and reaches about 25°N.

4 P-J PATTERN IN SUMMER

We also worked on similar calculation to investigate the P-J wave pattern. Figures 5 and 6 show the distribution of the first two EOF eigenvectors during June–July (Pentads 31–42) and July–August (Pentads 37–48), respectively. The variance contribution is presented in Table 2. Nitta^[8] pointed out that the P-J wave generally starts around the Philippines and then propagates northeastward. Similar to Figs. 1 and 2, the research area was chosen in the East Asia-Pacific region for the P-J pattern. This is

because EOF tends to display a wave signal in the limited area where P-J pattern occurs frequently. The other reason for the selected area is to weaken the OKJ wave signal. The variance contribution of the first three EOFs is shown in Table 2. A big positive center in the first eigenvector is located in North Pacific in high-latitudes and a negative one is to the southeast of the positive center during June–July. As a wave propagation, these west-east coherent centers are originating from the upstream area. However, it is much different from the OKJ wave shown in Fig. 1a. The spatial pattern in EOF II in Fig. 5b displays the “+ – +” correlation centers, which are located around the sea area near Southeast Japan, the Bering Sea and Gulf of Alaska respectively. The path of the connecting line of the correlation centers is similar to the great circle path described by Nitta^[8], indicating the typical distribution of the P-J wave pattern. A wave train structure of the third eigenvector (figure not shown) is distributed from the Northeast Asia to the central Pacific, which accounts for only 10.7% of the total variance. It should be noted that the variance contribution of the first eigenvector is relatively large (0.246). The variance contribution of the second eigenvector (0.177) is equivalent to that of the OKJ

wave in Fig. 1a.

The distribution of each eigenvector during July-August resembles that for June-July, and the coherent centers with large amplitudes in the first eigenvector are positioned over North Pacific in high latitudes. The distribution of the third eigenvector is similar to that of the OKJ wave distribution only with a slight phase drift (figure not shown). Figure 6b shows the typical distribution of P-J wave pattern, in which correlation centers almost overlap those in Fig. 5b. Its variance distribution is 0.178, which is close to that of

the second eigenvector for June-July (0.177).

Table 2. Variance contribution of the previous three eigenvectors in East Asia-Pacific area

Eigenvector	EOF I	EOF II	EOF III
June-July	0.246	0.177	0.107
July-August	0.196	0.178	0.114

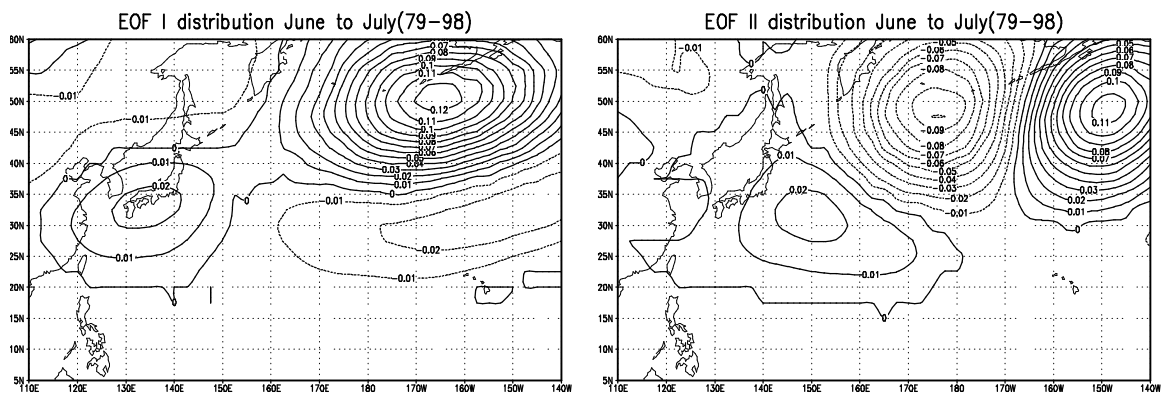


Fig. 5. Distribution of the previous two eigenvectors during June-July (Pentads 31-42) of the geopotential height at 500hPa (Z500) over East Asia- Pacific area

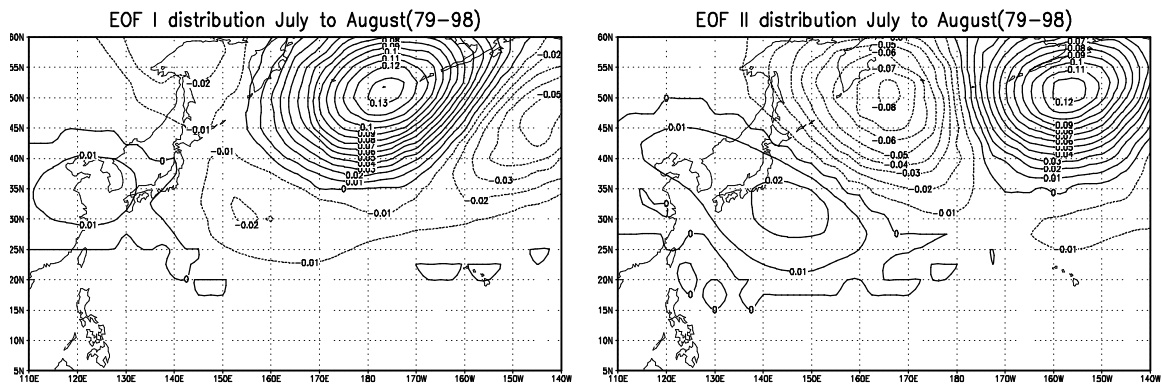


Fig. 6. Same as Fig. 5 except for the distribution during July-August (Pentads 37-48)

Above all, although the P-J wave train is not shown in the first principal component, its signal appears rather strong during the whole summer with variance contribution equivalent to that of the OKJ wave during June-July. In order to further study the P-J wave train, we examined the composite analysis of the second eigenvector of June-July and July-August respectively, although both of the distribution and variance contribution of the second eigenvector are nearly the same. Figure 7 shows the evolution of the coefficient of the second component during the two periods. Figures 8a and 8b show the composites of the horizontal wave activity flux and Z500 for the pentads over 1.0 (Fig. 8a) and below -1.0 (Fig. 8b) of the time coefficient of the second component during June-July, respectively. Figure 9 shows the composites during

July-August when the pentad coefficient is over 0.8 and below -0.8.

The situation of Z500 in Fig. 8a is similar to that in Fig. 9a. However, the subtropical high (5880 gpm contour) during June-July is located farther southwestward than that during July-August. The northeastward propagation of wave activity flux for the two periods also has their own features: The former originates from the Philippine Sea (about 25°N, 157.5°E) while the latter just starts from the Philippines and then propagates northeastward joining a southeastward flux at the area off the east coast of Japan. Obviously the northeastward wave flux represents the path and magnitude of the P-J wave train propagation. It should be noted that the southeastward OKJ-like propagation wave flux (Fig. 8a and 9a)

originates from the Sea of Okhotsk and merges into the P-J wave at mid-latitudes (about 40°N). The distribution of Z500 and wave activity flux in Figs. 8b & 9b are close to each other and in the same phase. The subtropical high (5880 gpm line) in Fig. 9b moved farther northeastward than that in Fig. 9a and the phase of the trough and ridge in Fig. 9b was basically opposite to that in Fig. 9a. The distribution of wave activity flux and the configuration of 500 hPa geopotential height in Fig. 9b are closer to the original P-J wave train proposed by Nitta^[8]. When convective activity becomes strong around the Philippines,

cyclonic circulation appears in situ; accompanying the northeastward P-J wave propagation, a reinforcement of the northeastern part of the subtropical high is found in Fig. 9b as pointed out by Nitta^[8]. This kind of changed circulation can bring warm summer to Japan and drought to China^[9]. Additionally, the wave flux propagation originating from the Okhotsk to the sea area off the east coast of Japan is not found, but more or less of the OKJ-like wave activity flux exists in Fig. 8b, which is also one of the distinctions between the two figures.

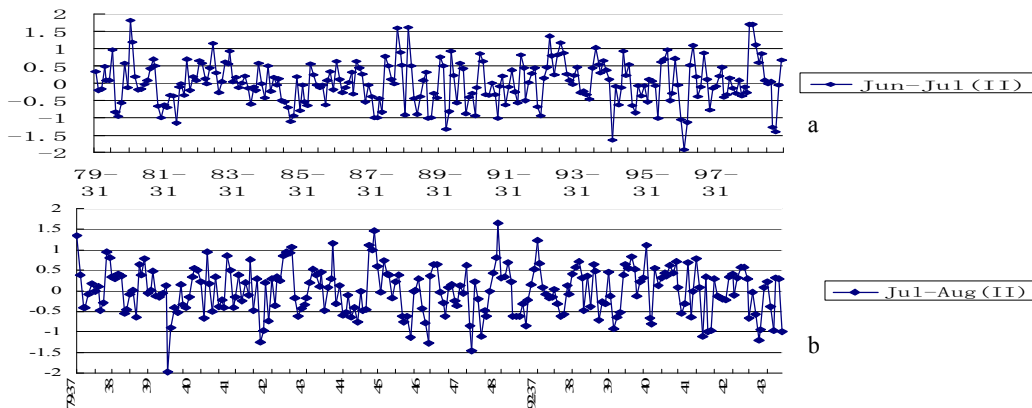


Fig. 7. Evolution of the coefficients matching Fig. 5b (a) and Fig. 6b (b)

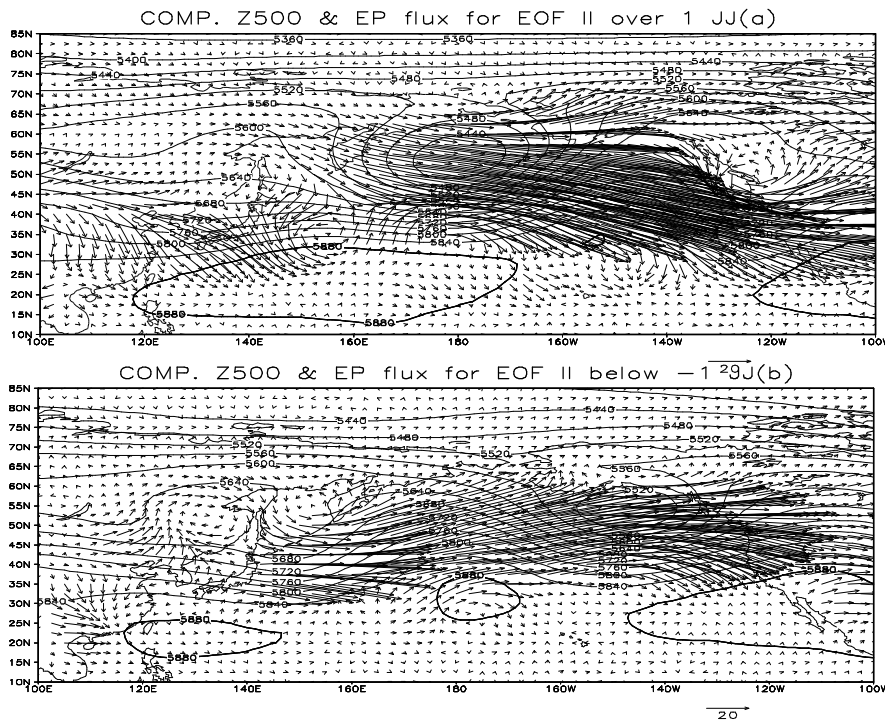


Fig. 8. The pentad composite distribution of Z500 and wave activity flux for the time series in Fig. 7a over 1 (a) and below -1 (b)

5 DISCUSSIONS AND SUMMARY

This study discussed the two teleconnection patterns and their related wave train propagations that often occur in the East Asian summer. Nevertheless,

the OKJ and P-J patterns play a very important role in affecting the weather in East Asian summer according to the current analysis. As analyzed with EOF, the OKJ wave and P-J wave are all very active during the whole summer and have their own distinctive feature.

The OKJ wave is basically the most significant distribution pattern in the Eurasia region during June–July and weakens dramatically, especially after August. On the other hand, the P–J wave train originating from Southeast Asia via the Pacific is the second primary distribution pattern during June–August. However, its variance contribution being equivalent to the former indicates that the P–J wave is active during the whole summer. Another interesting fact is that the P–J wave is related with the OKJ wave (Figs. 8a, 8b & 9a), which implies that the OKJ wave is also active during the whole summer. The signal of the OKJ wave to mid-summer (July–August) is, nevertheless, presented, as shown in Fig. 9a, with the opposite phase of the P–J wave proposed by Nitta^[8]. The OKJ wave signature disappeared completely only with the positive P–J wave phase in late summer (Fig. 9b). Wang^[14] once pointed out that the two wave trains can join together in the area east of Japan, which indicates a possible interaction between the two wave trains. The coexistence of the two wave trains can be found in Figs. 8 & 9a. Due to the different occurrence region of the two wave trains, the EOF failed to separate the two wave trains completely in East Asia-Pacific region during July–August (as shown in Fig. 9a). The frequent occurrence of the OKJ wave with the development of the blocking high around Sea of Okhotsk probably results from global warming^[15]. Consequently, the study about the occurrence frequency and interaction between the two wave trains is improving our understanding of the climate over East Asia and the whole world as well.

This study examines the wave trains at 500 hPa by using EOF analysis as a diagnostic tool and in combination with the diagnosis analysis. Current results are as follows:

(1) The OKJ pattern originating from the upstream areas of the Sea of Okhotsk to the subtropical regions could display its strong signal in early and middle summer. The OKJ pattern is clearly recognized in the first EOF component in Eurasia.

(2) The P–J pattern shows quite strong signals in the whole summer. Although the P–J pattern is described as the second EOF component around the area from East Asia to Northeast Pacific ocean, the variance contribution is the same as that of the OKJ pattern in the first EOF component.

(3) Except for the P–J wave activity flux as the mainstream shown in Figs. 8a, 8b & 9a, we can find a southeastward propagation of wave flux (OKJ-like) which originates from the upstream area of the Sea of

Okhotsk and intersects with the P–J like wave flux in the sea area off the east coast of Japan. Thus, the composite analyses indicate that the OKJ and P–J wave trains could coexist to some extent.

REFERENCES:

- [1] WALKER G T, BLISS E W. World weather [J]. V Mem. R Meteor. Soc., 1932, 4(2): 53-84.
- [2] WALLACE J M, GUTZLER D S. Teleconnection in the geopotential height field during the Northern Hemisphere winter [J]. Mon. Wea. Rev., 1981, 109(4): 784-812.
- [3] HOSKINS B J, KAROLY D J. The steady linear response of a spherical atmosphere to thermal and orographic forcing [J]. Atmos. Sci., 1981, 38(6): 1 179-1 196.
- [4] WANG Y. Effects of blocking anticyclones in Eurasia in the rainy season (Meiyu/Baiu season) [J]. J. Meteor. Soc. Japan, 1992, 70(5): 929-951.
- [5] KATO K. The synoptic features about the Okhotsk high related to YAMASEI [R]// KISHOU-KENKYU (Meteorological Research) Note, Tokyo: Meteorological Society of Japan, 1995, 183: 67-69.
- [6] NAKAMURA H, et al. The evolution of blocking and its dynamics related with the formation of Okhotsk high [R]// KISHOU-KENKYU (Meteorological Research) Note, Tokyo: Meteorological Society of Japan, 1997, 189: 177-190.
- [7] OGI M, TACHIBANA Y, YAMAZAKI K. The connectivity of the winter North Atlantic oscillation (NAO) and the summer Okhotsk High [J]. J. Meteor. Soc. Japan, 2004, 82(3): 905-913.
- [8] NITTA T. Convective activities in the tropical western Pacific and their impact on the northern hemisphere summer circulation [J]. J. Meteor. Soc. Japan, 1987, 65(3): 373-390.
- [9] HUANG R H, LI W J. Influence of the heat source anomaly over the western tropical Pacific on the subtropical high over East Asia [C]// Proc. International conference on the general circulation of East Asia (Tokyo), 1987: 40-51.
- [10] PIUMB R A. On the three dimensional propagation of stationary waves [J]. J. Atmos. Sci., 1985, 42: 217-229.
- [11] OVERLAND J E, PREISENDORFER R W. A significance test for principal applied to a cyclone climatology [J]. Mon. Wea. Rev., 1982, 110(1): 1-4.
- [12] WANG Y, YASUNARI T. A diagnostic analysis of the wave train propagating from high-latitudes to low-latitudes in early summer [J]. J. Meteor. Soc. Japan, 1994, 72(2): 269-279.
- [13] WANG Y, WANG B, OH J H. Impact of the preceding El Nino on the east Asian Summer Atmospheric Circulation [J]. J. Meteor. Soc. Japan. 2001. Vol.79. No.1B: 575-588.
- [14] WANG Y, FUJIYOSHI Y, KATO K. A teleconnection pattern related with the development of the Okhotsk high and the northward progress of the subtropical high in East Asian summer [J]. Adv. Atmos. Sci., 2003, 20(2): 237-244.
- [15] WANG Ya-fei, TAKAHASHI K. Decadal climate variability of rainfall around the middle and lower reaches of the Yangtze River and atmospheric circulation [J]. J. Trop. Meteor. (in Chinese), 2005. 21 (4): 351-358.

Citation: WANG Ya-fei, HE Jin-hai, LI Yan et al. An empirical orthogonal function analysis for the wave trains in East Asian summer. *J. Trop. Meteor.*, 2010, 16(3): 231-237.